Influence of Stream-Subsurface Exchange Flux and Bacterial Biofilms on Oxygen Consumption Under Nutrient-Rich Conditions

Original
Influence of Stream-Subsurface Exchange Flux and Bacterial Biofilms on Oxygen Consumption Under Nutrient-Rich Conditions / De Falco, N., Boano, F., Bogler, A., Bar-Zeev, E., Arnon, S.. - In: JOURNAL OF GEOPHYSICAL RESEARCH. BIOGEOSCIENCES. - ISSN 2169-8953. - ELETTRONICO. - (2018). [10.1029/2017JG004372]

Publisher:
American Geophysical Union

Published
DOI:10.1029/2017JG004372

AGU100 ADVANCING EARTH AND SPACE SCIENCE

JGR

Journal of Geophysical Research: Biogeosciences

RESEARCH ARTICLE

10.1029/2017JG004372

Key Points:

- Biomass distributions varied within 1 order of magnitude across the bed forms and were not strongly correlated with oxygen consumption rates
- Oxygen consumption rates varied over 4 orders of magnitude and were dependent on the vertical exchange flux at the water-streambed interface
- Main bacterial taxonomic classes were similar across bed forms despite variations in flow conditions and sediment disturbance events

Supporting Information:

- Supporting Information S1

Correspondence to:
S. Arnon,
sarnon@bgu.ac.il

Citation:
De Falco, N., Boano, F., Bogler, A., Bar-Zeev, E., & Arnon, S. (2018). Influence of stream-subsurface exchange flux and bacterial biofilms on oxygen consumption under nutrient-rich conditions. *Journal of Geophysical Research: Biogeosciences*, *123*. https://doi.org/10.1029/2017JG004372

Received 20 DEC 2017
Accepted 1 JUN 2018
Accepted article online 20 JUN 2018

Influence of Stream-Subsurface Exchange Flux and Bacterial Biofilms on Oxygen Consumption Under Nutrient-Rich Conditions

N. De Falco[1], **F. Boano**[2], **A. Bogler**[1], **E. Bar-Zeev**[1], **and S. Arnon**[1]

[1]Zuckerberg Institute for Water Research, Jacob Blaustein Institutes for Desert Research, Ben-Gurion University of the Negev, Beersheba, Midreshet Ben Gurion, Israel, [2]Department of Environment, Land and Infrastructure Engineering, Politecnico di Torino, Turin, Italy

Abstract The lack of a complete understanding of the complex reciprocal interactions between hydrological processes and the structure and function of microbial communities limits our ability to improve the predictions of microbial metabolism in streams. We report here on how overlying water velocity and losing and gaining flux interact with bacterial community structure and its activity to control oxygen consumption in a sandy streambed under high nutrient levels. We used an experimental flume packed with natural sediment and measured the bacterial biomass distribution and oxygen profiles in the streambed and across bed forms. Local oxygen consumption rates were calculated with a 1-D numerical model (GRADIENT). Bacterial abundance and production rates varied across the bed form within 1 order of magnitude, while their taxonomic classes were similar across bed forms despite variations in flow conditions and sediment disturbance events. However, bacterial production rates were not directly correlated with bacterial abundance. On the other hand, oxygen consumption rates ranged over 4 orders of magnitude across the bed forms and were highly correlated with the vertical exchange flux between the water and the streambed. The results strongly suggest that under high nutrient levels, the system is, in general, transport limited and that predicting oxygen consumption rates depends on local vertical exchange fluxes.

1. Introduction

Recent studies have illustrated the importance of stream networks to global nutrient cycling, which far exceeds their relatively minor surface coverage of the terrestrial environment (Marx et al., 2017; Raymond et al., 2013; Zscheischler et al., 2017). The ability of streams to recycle nutrients at much greater turnover rates than other terrestrial and aquatic environments is due to their fast water flow and exchange processes, which bring water and nutrients into contact with a shallow sedimentary environment that is rich in biomass (Bardini et al., 2012; Battin et al., 2008). The process of water and nutrient exchange back and forth across the streambed interface is commonly termed hyporheic exchange (Boano et al., 2014), and the active ecotone between the surface stream and the groundwater is called the hyporheic zone (Boulton et al., 1998).

Hyporheic exchange is influenced by numerous factors including stream water velocity, morphological structures, streambed characteristics, and interactions with groundwater. (Boano et al., 2014; Cardenas, 2015). For example, Gomez-Velez & Harvey (2014) and Gomez-Velez et al. (2015) illustrated that hyporheic exchange flux along stream networks is dominated by bed forms rather than by other morphological structures such as meanders and alternate bars. Other studies have shown that in dune-shaped bed forms, the interaction between stream water velocity and the groundwater controls hyporheic exchange in a complex manner (Cardenas, 2009; Fox et al., 2014; Packman et al., 2004). On the one hand, hyporheic exchange increases proportionally to the square of the stream water velocity (Arnon et al., 2007; Packman et al., 2004). On the other hand, increasing vertical flux in the form of net losing or gaining streams, regardless of the flow direction, reduces hyporheic exchange flux, as well as the size of the hyporheic zone (Cardenas, 2009; Fox et al., 2014, 2016; Packman et al., 2004). Ultimately, the resulting net exchange flux between the stream and the hyporheic zone depends on the combination between the hyporheic exchange flux driven by the overlying water velocity and the vertical flux caused by the interaction with the groundwater. The exchange flux further influences solute transport (Fox et al., 2014, 2016), the movement and deposition of suspended fine particles (Fox et al., 2018; Partington et al., 2017), various conditions in ecological habitats (Boulton et al., 2010; Mathers et al., 2014), and biogeochemical reaction rates (De Falco et al., 2016; Newcomer et al., 2018).

Biogeochemical processes are of particular interest due to the active role of microorganisms, which constitute the base of the aquatic food web. Heterotrophic bacteria can hydrolyze and assimilate dissolved organic carbon (DOC) via catabolism while consuming oxygen through aerobic respiration (Newcomer et al., 2018). Thus, oxygen consumption is often used to evaluate bacterial activity since aerobic respiration is the most energy-efficient metabolic process. Transfer of oxygen typically occurs from the stream water to the streambed; thus, oxygen consumption in the hyporheic zone often results in a gradient of oxygen from the surface and along the flow path within the streambed (Caruso et al., 2017). Bacteria, as well as sessile microbial communities (referred to hereafter as biofilm), also utilize other nutrients at high rates for metabolism and proliferation. Concurrently, biofilm growth may also reduce the pore space, thus influencing the flow patterns and water flux due to clogging (Higashino, 2013; Samsó et al., 2016). Clogging can also occur through the formation of methane and N_2 gas bubbles via bacterial denitrification (Baveye et al., 1998; Flury et al., 2015).

Hydrological and microbiological processes in the hyporheic zone have been studied extensively in the last four decades, emerging from the early works by Bencala and Walters (1983) and others (see review by Cardenas, 2015). Hydrological and microbiological studies were initially independent. However, current research acknowledges the need to develop a multiprocess and multiscale understanding, specifically related to biogeochemistry (Cardenas, 2015). Namely, the influence of the microbial biomass and community structure on biogeochemical processes is not independent of hydrology, and hydrological processes are affected by the dynamics of the biomass and microbial community structure (e.g., Mendoza-Lera et al., 2017).

Despite the increasing appreciation of hydrological and microbiological bidirectional interactions, they are still missing from many quantitative frameworks, partly due to the lack of process understanding. For example, clogging has been frequently addressed in recent years but mostly only through modeling studies with very few direct measurements of biofilm community structure and spatial distribution (Caruso et al., 2017; Mendoza-Lera & Mutz, 2013; Newcomer et al., 2018). Other studies showed that disturbances, such as sediment mixing due to high flow events or bioturbation, can restore the hydraulic conductivity of a clogged bed, sometimes without reducing microbial respiration rates (Mendoza-Lera & Mutz, 2013; Nogaro et al., 2006). In another study, Aubeneau et al. (2016) showed that biofilm development reduced hyporheic exchange; however, the residence time of water within the hyporheic zone was extended.

The bidirectional interactions between hydrological and microbiological processes also play an important role in microbial communities' shape and composition. For example, flow patterns control the nutrient supply, which impacts community composition (Besemer et al., 2007; Hödl et al., 2013). Shear forces at the stream sediment interface affect not only microbial communities but also the biofilm architecture (Hödl et al., 2013; Risse-Buhl et al., 2017). While complex microbial communities of benthic biofilms are composed of bacteria, archaea, protists, fungi, and algae, many studies focused on subgroups of these organisms either to simplify experimental methods or in order to examine a specific process that is only relevant for a specific type of organism. For example, many studies focused on bacteria because they are the most abundant group of organisms (Besemer et al., 2012).

Despite all the above mentioned studies, there is still a major gap in understanding the coupling between microbial aspects (e.g., abundance and community structure) and hydrological forcing (water flux, hydraulic conductivity, etc.). In this research, we used controlled flume experiments to systematically study how the exchange flux between the stream and the streambed, as well as bacterial abundance and community structure, interacts with each other and how these interactions control oxygen consumption rates under nutrient-rich conditions. It was hypothesized that under these conditions, biomass accumulation will reach a certain level at which no significant growth will occur, and oxygen consumption rates will be dictated by its delivery into the bed. In addition, bacterial community structure will be spatially distributed when different physical conditions prevail along the bed forms, but this distribution will not be a significant factor controlling local oxygen consumption rates. Such nutrient-rich conditions are typical of streams and rivers that receive treated wastewater or other point source pollution.

2. Materials and Methods

2.1. Experimental System

The effects of flow conditions and biomass distribution on oxygen consumption were studied using a 260-cm-long and 29-cm-wide recirculating indoor flume (Figure 1). The circulation of water in the channel

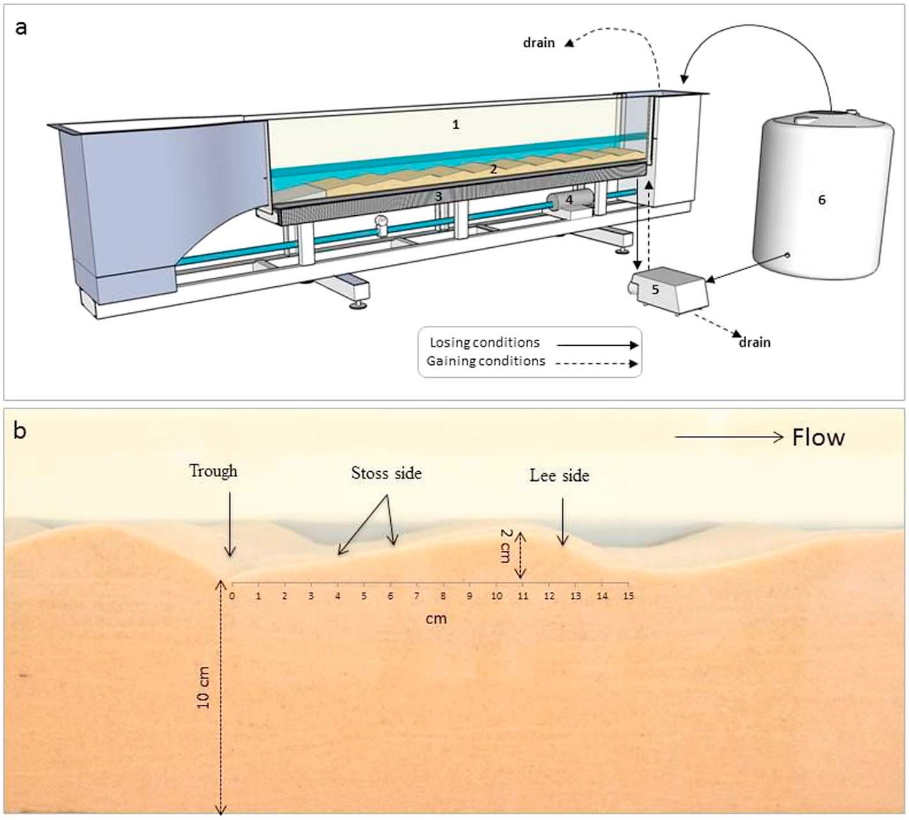

Figure 1. Schematic illustration of the experimental setup for studying oxygen consumption (a) and an illustration of a representative bed form before biofilm growth (b). Arrows in panel b show the locations of biomass sampling and oxygen profiling (see sections 2.3 and 2.4). The numbers indicate the main channel (1), the sand bed (2), the drainage/injection system (3), the centrifugal pump for driving the flow in the channel (4), the peristaltic pump for imposing losing or gaining flow conditions (5), and the reservoir for storing fresh water for injecting into the flume under gaining conditions (6).

was driven by a variable speed pump, and the discharge was measured with a magnetic flow meter located in the return pipe (SITRANS MAG 5100, Siemens, Germany). A drainage system was placed on the bottom of the flume channel and was connected to a peristaltic pump (Masterflex 7523-80, Cole Parmer, United States), which enabled the magnitude of losing or gaining fluxes to be controlled (Fox et al., 2014). Deionized water with 100% saturation of oxygen was injected from the drainage system under gaining conditions, while water was pumped out from the drainage system under losing conditions. In order to maintain the same volume of water in the flume system, water was pumped out from the main channel under gaining conditions and added from a separate tank under losing conditions (De Falco et al., 2016). Losing and gaining fluxes (q_L and q_G, respectively) were calculated as the discharge imposed by the peristaltic pump per unit bed area. Water in the flume was kept at a constant temperature of 25 °C using a chiller (TR/TC 10, TECO Refrigeration Technologies, Ravenna, Italy). Oxygen concentration in the stream water was maintained at 80–100% saturation by forcing air through a diffuser in the flume's outlet chamber (AFD-270, 9″, SSI Aeration, NY, United States). The flume was covered with a black cloth during the entire experimental period to minimize photosynthesis and prevent algal growth.

2.2. Sediments

The flume was packed with fine sand collected from the Yarqon Stream, a perennial stream located in the central part of Israel (Arnon et al., 2015). This sand was sieved (2 mm) to remove large particles and branches and immediately packed into the flume. The sediments were manually arranged in dune-shaped bed form structures of 15 cm in length and 2 cm in height (Figure 1b). The bed form height and wavelength were uniform across the width of the flume. The average water depth was measured from the water surface to the mean bed level and was 7 cm, while the average depth of the bed was 11 cm. The bed material was uniform and composed of fine sand (D_{50} = 140 μm) with a hydraulic conductivity of 0.0197 cm/s (Klute & Dirksen, 1986). To ensure diverse DOC sources, we added to the water dried organic matter by spreading 116 g of dried Cyanophita (desiccated at 65 °C for 24 h) and 12 g of *Populus tremula* fresh leaves. A micronutrient solution was also added to the flume water several times during the acclimation phase. The solution included (mg in 400 L): 400 $Ca(NO_3)_2\ 4H_2O$, 248 KH_2PO_4, 500 $MgSO_4\ 7H_2O$, 316 $NaHCO_3$, 45 EDTA Na_2, 49.6 H_3BO_3, 278 $MnCl_2\ 4H_2O$, 60 $NaMoO_4\ 2H_2O$, 0.8 Cyanocobalamin (B_{12}), 0.8 Thiamine HCL, 1140 $NaSiO_3\ 9H_2O$, 0.8 Biotina, 1.2 $CoCl_2\ 6H_20$, 60 $ZnSO_4\ 7H_2O$, and 12 $CuSO_4\ 2H_2O$.

2.3. Oxygen Profiling

The vertical distribution of oxygen concentrations in the streambed was measured at four different locations across a single bed form (0, 4, 6, and 12 cm from the trough, Figure 1b). The oxygen profiles were measured under different combinations of overlying water velocities (4 and 10 cm/s) and subsurface fluxes (q_L and $q_{G,}$ of 20 and 50 cm/day, respectively, and under neutral flow conditions in which no vertical flux was imposed). Data acquisition began by setting the flow conditions to the required values in the evening before the oxygen profiles were measured. Profiling was done the next day and 2 h after spiking the bulk water with a feed solution to ensure that there was no nutrient limitation. The feed solution contained 6.8 g $NaC_7H_5O_2$ (sodium benzoate), 14 g KNO_3, and 0.5 g KH_2PO_4, which resulted in a C:N:P molar ratio of 106:16:1. Waiting more than 2 h after spiking with the nutrient solution did not yield different oxygen profiles. During profiling, labile DOC in the bulk water was maintained at 8–10 mg/L by adding sodium benzoate.

Oxygen profiling was initiated 2 weeks after packing the sand in the flume to allow for biofilm acclimation. This acclimation phase was achieved under neutral conditions at an overlying water velocity of 10 cm/s, which was less than what is required to cause sand movement (> 20 cm/s). The first data set is referred to in the text as *disturbed* bed forms since we mimicked the effect of sediment mixing during bed form migration under a high flow event by manually mixing the upper 5 cm of sediment in the flume every evening before a measurement was conducted. The process was similar to that used by Gerull et al. (2012). While the manual mixing did not precisely mimic the physical structures that may develop during bed form migration, it did homogenize the microbial biomass distribution, which was the desired experimental outcome of this manipulation. After the data set was collected under all the above mentioned flow conditions, the flume was operated for an additional 2 months under neutral flow conditions at an overlying water velocity of 10 cm/s without sediment mixing. The same nutrient solution (6.8 g $NaC_7H_5O_2$, 14 g KNO_3, and 0.5 g KH_2PO_4) was added three times a week to support the acclimation to the new conditions, which are referred to as *stationary* bed forms. The oxygen profiling was repeated after this 2-month period to produce the data under stationary bed forms.

2.4. Biofilm Sampling

Biofilm samples were collected twice from three bed forms located in the central section of the flume, after each set of oxygen profiling was terminated. The sampling of the disturbed and stationary bed forms was done 1 and 3 months after packing the sediments in the flume, respectively. The sample collection was performed after the flow was stopped, the water level was lowered to the surface of the bed form, and autoclaved plastic rings (2.5 cm in diameter and 1 cm in height) were inserted into the sand. Wet sand from the entire volume of the ring (~10 g) was gently sampled using a sterile spatula (supporting information Text S1). This volume was large enough to include the depth of aerobic bacterial activity and to eliminate small-scale heterogeneity. In each of the four locations, a composite sample was obtained by collecting sand from three locations across the width of the bed forms. The sediment samples were divided to analyze bacterial abundance and production. The pore water content in each sample was measured to normalize the results to the dry weight of the sand. Sediment samples were also taken from the Yarqon Stream by scraping the upper 1 cm of sediment into sterile vials from the stoss and lee sides of two bed forms that were similar in shape and size to those packed in the flume.

2.5. Chemical and Biological Analysis

Oxygen concentration in the bulk water was measured using an optical oxygen sensor (WTW Multi340, GmbH, Weilheim, Germany). The oxygen profiles were measured using a Clark-type oxygen microelectrode, mounted on a micromanipulator with computerized depth control and a data acquisition system (Unisense, Aarhus, Denmark). The oxygen microelectrode had a tip diameter of 50 μm, a stirring sensitivity <2%, and a

90% response time < 5 s. The DOC concentrations in the bulk water were measured with an online UV/Vis spectrophotometer (Scan, Messtecnik GmbH, Brigittagasse, Austria), after calibration with a Total Organic Carbon analyzer (De Falco et al., 2016).

Bacterial abundance was determined by flow cytometry according to Frank et al. (2017). A sediment sample (1 ml) was collected from the flume and placed in a cryotube with 0.8 ml of autoclaved flume water and 6 μl of glutaraldehyde, snapped freezed, and kept at −80 °C. Prior to analysis, the samples were thawed (~25 °C) and mildly sonicated (Model CL-188, QSONICA LLC, United States) for 15 s with 5 mM of ethylenediaminetetraacetic acid to separate the bacterial cells from the sediment. Bacterial cells were then stained with 1 μl of SYBR green (Applied Biosystems cat #S32717), incubated for 10 min in the dark and analyzed by an Attune® acoustic focusing flow cytometer (Applied Biosystems) equipped with 488- and 405-nm lasers. For the size standard, 1-μm beads (Polysciences) were used.

Bacterial production rates were measured in triplicates according to Simon and Azam (1989) and Frank et al. (2017). Briefly, aliquots from each sample (2 ml of sediment) were incubated with 100 nmol^{-1} of [4,5-3H]-leucine (Perkin Elmer, United States) for 4 h at room temperature in the dark. The incubation time was halted by adding 100 μl of cold (4 °C) trichloroacetic acid (100%), followed by short centrifugation (10 min at 10,000 revolution per minute) (Smith & Azam, 1992). The samples (pellets) were analyzed using a TRI-CARB 2100 TR scintillation counter (Perkin Elmer, United States) following the addition of 1 ml of scintillation cocktail (Ultima-Gold, Quick-Safe A). The carbon assimilation rate was calculated using a conversion factor of 1.5 $\text{kg}\cdot\text{C}\cdot\text{mol}^{-1}$ with an isotope dilution factor of 2.0 (Simon & Azam, 1989). Controlled (blank) samples were determined following the addition of 100% trichloroacetic acid. Specific bacterial activity was calculated by dividing the bacterial production rates by the bacterial abundance.

Total genomic DNA was extracted using a PowerSoil® Kit (MoBio), with minor changes to the manufacturer's protocol. Briefly, a sediment sample (50 ml) was centrifuged (10,000 g, 2 min) to remove all the pore water. A subsample (250 μg) was then collected using a sterile spatula and added to the PowerBead Tubes. Finally, the DNA was eluted into the elution solution (50 μl) provided with the kit via two washing steps that included a short centrifugation (10,000 g for 30 s).

Library preparation, sequencing, and analysis were performed by Hy Laboratories Ltd. (hylabs, Israel). Sequence libraries were prepared using a two-step Polymerase chain reaction (PCR) protocol. In the first step, the V4 region of the 16 rRNA gene was amplified using primers 515F and 807R (Earth Microbiome Project), followed by a second PCR using the Fluidigm Access Array Primers for Illumina to add the adaptor and index sequences. Cleaning the second PCR was done by AMPure beads, and the generated libraries were quantified by Qubit and the size determined by Tapestation analysis. The libraries were then sequenced on an Illumina Miseq using the V2 kit for 500 cycles (250 × 2, paired end reads). Data analysis was performed using the CLC Bio Genomics Workbench and Microbial Module.

2.6. Data Analysis

Oxygen profiles were fitted with GRADIENT, a novel algorithm that evaluates the reaction rate distributions from observed steady state concentration profiles (Boano et al., 2018). GRADIENT is a Matlab code that extends a previously published framework relying only on diffusion (Berg et al., 1998) to include the role of nutrient advection. GRADIENT provides robust estimates of reaction rates in sediments with significant vertical water flow. The fit between modeled and observed oxygen concentrations yielded an optimal depth distribution of reaction rates, which was then integrated over depth to express the rates as $\mu g\ O_2/cm^2$ day. The model calculates a reaction rate directly from a simple mass balance approach without any assumptions about reaction kinetics or biomass amount. For the boundary conditions, concentrations at the upper and lower boundaries were set to equal the observed concentration values. Applying GRADIENT here depended on knowing the local value of the vertical water flux at the streambed surface, which was determined with a modified version of the hydraulic model developed by Bardini et al. (2012).

The effects of fluxes (fixed variables), the bed form type (stationary versus disturbed; fixed variables), and the random effect of the location in the bed form on oxygen consumption rates were evaluated by a three-way analysis of variance (ANOVA). Normality was met through square root (SQRT) transformation. The ANOVAs were followed by a pairwise post hoc Tukey honestly significant difference to evaluate significance ($p < 0.05$). The effects of location and bed form type on bacterial abundance, bacterial production rates,

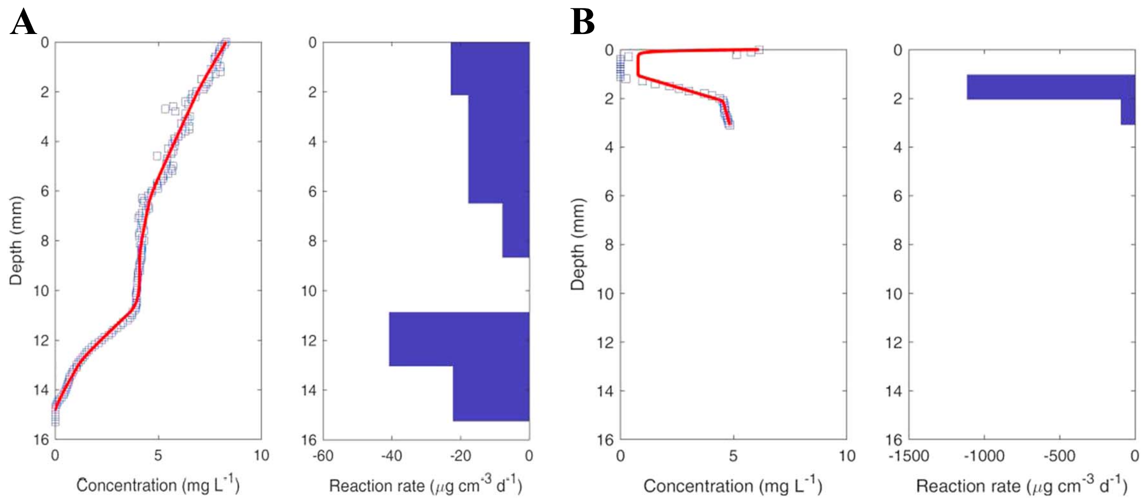

Figure 2. Measured (squares) and fitted (solid lines) oxygen profiles with their corresponding vertical distribution of oxygen consumption rates in the sediment (bars). The two cases shown represent disparate flow conditions spanning over a wide range of r^2 as shown in Table 1. (a) Results from the case of a *disturbed* bed form, neutral conditions, v = 10 cm/s (r^2 = 0.99). (b) The case of a *stationary* bed form, gaining conditions q_G = 20 cm/day, v = 4 cm/s (r^2 = 0.66). Note that the reaction rates in the two graphs have different scales.

and cell-specific activity were evaluated with a two-way ANOVA. Normality was met using a 1/SQRT for the bacterial abundance data and by SQRT transformation for bacterial production rates and cell-specific activity. The ANOVAs were followed by Tukey's post hoc test to test for significant differences between treatments ($p < 0.05$). A multiple linear regression analysis was done between oxygen consumption rates and the different microbiological and hydrological variables including microbial abundance, bacterial production rates, overlying water velocity, imposed vertical flux, and modeled vertical flux. We conducted a model selection analysis based on the Akaike information criterion, AIC (Akaike, 1973). All statistical tests were conducted using Statistica 12.5 (StatSoft Inc., Tulsa, OK, United States).

3. Results

Oxygen distribution within the streambed and across the bed form under the different flow conditions yielded a set of disparate oxygen profiles. Each profile was analyzed with GRADIENT to compute the local consumption rate. Two representative profiles highlight the range of goodness of fit between the measured

Table 1
Oxygen Consumption Rates (μg O_2/cm^2 day) Across the Bed Forms Under Different Flow Conditions

Experimental conditions	Location in the bed form	Losing 50 cm/day	Losing 20 cm/day	Neutral 0 cm/day	Gaining 20 cm/day	Gaining 50 cm/day
Disturbed bed forms v = 4 cm/day	0	635.9 (0.86)	240.2 (0.99)	No fit	No fit	61.3 (0.10)
	4	390.5 (1)	138.2 (0.99)	1.55 (0.99)	No fit	No fit
	6	356.8 (0.99)	140.0 (0.99)	4.38 (0.99)	No fit	85.5 (0.29)
	12	295.5 (0.99)	112.3 (0.99)	0.42 (0.94)	No fit	18.9 (0.08)
Disturbed bed forms v = 10 cm/s	0	347.3 (1)	203.9 (0.99)	No fit	No fit	No fit
	4	188.4 (0.93)	133.1(0.99)	10.4 (0.94)	No fit	No fit
	6	197.0 (0.93)	123.6 (0.98)	28.1 (0.99)	No fit	No fit
	12	289.4 (0.98)	62.6 (0.98)	No fit	No fit	No fit
Stationary bed forms v = 4 cm/s	0	493.3 (0.92)	218.6 (0.97)	5.2 (0.99)	141.7 (0.66)	191.8 (0.80)
	4	216.9 (0.41)	140.0 (0.98)	4.83 (0.87)	40.5 (0.27)	165.9 (0.95)
	6	318.0 (0.85)	133.9 (0.96)	8.53 (0.99)	64.0 (0.87)	222.9 (0.87)
	12	268.6 (0.98)	100.2 (0.98)	8.32 (0.96)	70.3 (0.83)	148.6 (0.87)
Stationary bed forms v = 10 cm/s	0	559.9 (0.97)	189.2 (0.90)	No fit	No fit	260.1 (0.89)
	4	353.4 (0.89)	133.9 (0.96)	18.7 (0.87)	No fit	116.6 (0.85)
	6	309.3 (0.91)	139.1 (0.78)	26.3 (0.63)	45.3 (0.90)	165.0 (0.86)
	12	309.3 (0.98)	109.7 (0.99)	12.7 (0.98)	80.3 (0.94)	234.1 (0.86)

Note. Goodness of fit for each model fit is expressed as r^2 and appears in parentheses.

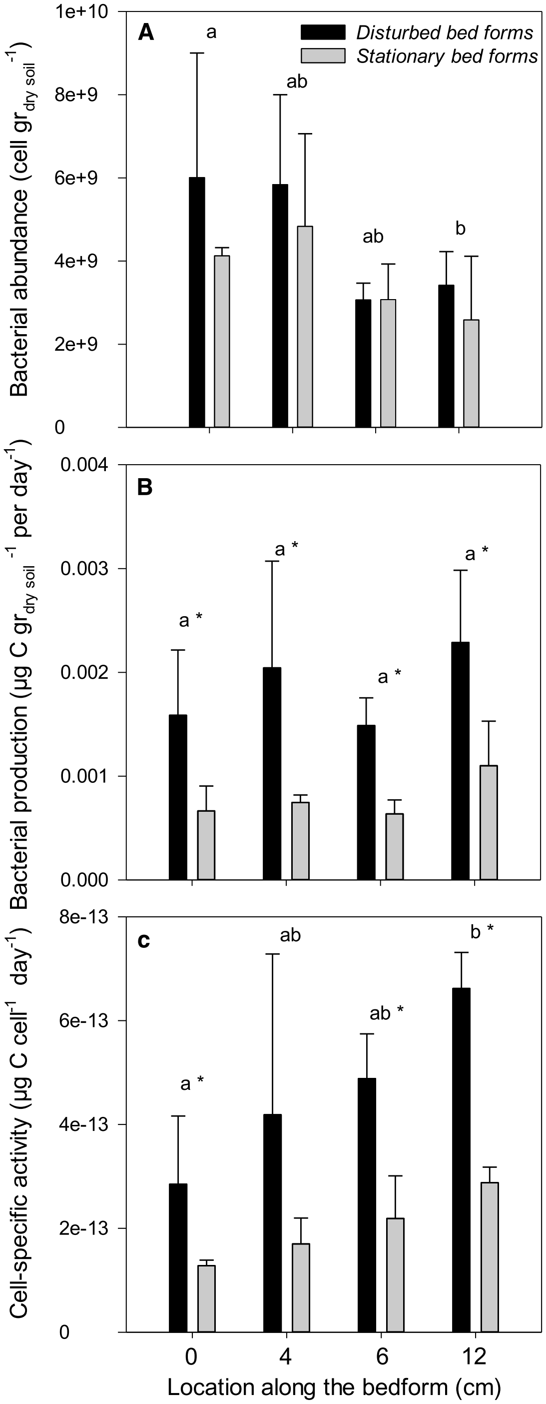

Figure 3. Bacterial abundance (a), bacterial production (b), and cell-specific activity (c) across the bed forms. Sampling was conducted twice, at the end of each experimental phase, representing the *stationary* bed forms and *disturbed* bed forms. Results are based on the average values ± standard deviations of three bed forms located 113, 128, and 143 cm from the flume inlet. Lowercase letters (a, b) indicate significant differences between locations, while asterisks mark significant differences between disturbed and stationary bed forms ($p < 0.05$).

oxygen concentrations and the modeling results in which consumption rates were determined (Figure 2). The oxygen consumption rates from all the profiles are displayed in Table 1. Since most of the consumption took place in a relatively thin layer at the top of the streambed (from a few millimeters down to 1.5 cm), using a 1-D model is a powerful approach since it is simple to run while providing robust results (Boano et al., 2018). In general, the depth of the active zone was deeper under losing flow conditions than under gaining conditions (Figure 2). Also, a better fit was achieved under losing and neutral flow conditions than that achieved under gaining conditions. No fit was reported when GRADIENT could not converge during the calculations (Table 1). The lowest oxygen consumption rates were found under neutral conditions, and they increased when the losing or gaining fluxes increased ($p < 0.05$). The oxygen consumption rates were also significantly different ($p < 0.05$) between the disturbed and stationary bed forms. However, under all tested conditions, oxygen consumption rates were similar across the individual bed forms ($p > 0.05$).

The water reservoir that was used to feed the upwelling water under gaining conditions was saturated with oxygen but did not contain nutrients. While some oxygen consumption occurred during flow in the lower section of the bed, we only accounted for the activity in the top layer of the bed. Thus, the upwelling water that was included in our analysis represents groundwater deprived of nutrients and oxygen, as shown, for example, in the oxygen profile in Figure 2b.

The results in Table 1 indicate that flow conditions and bed form type had significant effects on oxygen consumption rates, while location had a smaller impact. Concurrently, bacterial abundance, bacterial production rates, and cell-specific activity were measured following the oxygen profiling to evaluate the importance of bacterial distribution and metabolism (Figure 3). Bacterial abundance did not differ between bed form types (disturbed versus stationary, Figure 3a, $p > 0.05$). However, the bacterial abundance distribution across the bed form was heterogeneous, with significantly more bacteria found in the trough than on the lee side of the bed form (Figure 3a). Bacterial production rates, which illustrate the assimilation rates of carbon by microbial biofilm as defined by Simon and Azam (1989), were significantly higher in the disturbed bed forms than in the stationary bed forms but not across the bed form (Figure 3b). Such carbon assimilation illustrates how much carbon is incorporated into the biomass, not including respiration. Due to the different trends shown in bacterial abundance and bacterial production rates, we combined the information to yield the cell-specific activity in order to better explore the metabolic differences between communities (Figure 3c). Differences in cell-specific activity across the bed form were found only between the trough and the lee side, but the trends were the opposite of that of bacterial abundance, with the maximum cell-specific activity found on the lee side. Differences between bed form types were found at three locations but not on the stoss side at the location of 4 cm (Figure 3c). Interestingly, the cell-specific activity showed a trend of increasing rates across the bed form (from location 0 to 12 cm), regardless of the type.

The biofilm community structure across the disturbed bed form, which was mixed on a daily basis for about 2 weeks, was similar (Figures 4a and 4b). In addition, the community in the disturbed bed form was similar to

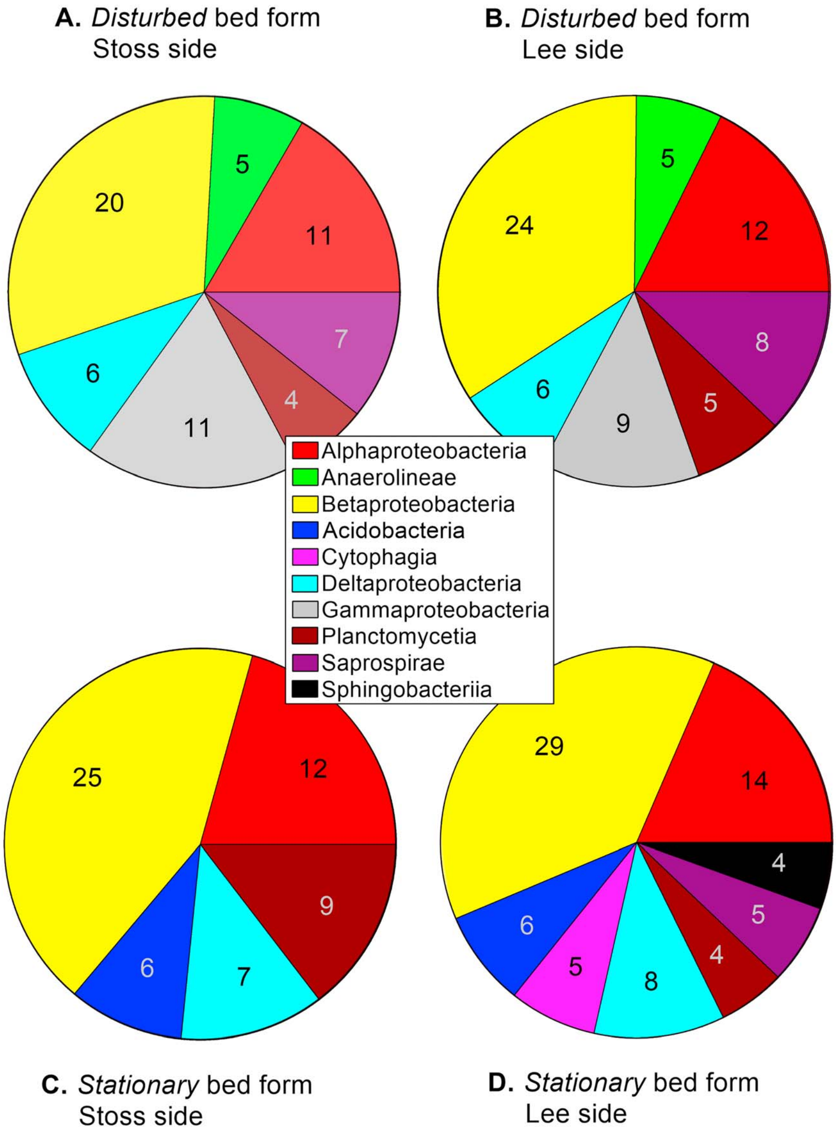

Figure 4. Bacterial community structure from *disturbed* (a, b) and *stationary* (c, d) bed forms that were sampled on the stoss side (a, c) and the lee side (b, d) of the bed forms. Only bacterial classes that represent more than 4% operational taxonomic units were included in the figure. Numbers indicate the percent of operational taxonomic unit abundance for each class. Acidobacteria was represented in the flume by the Chloracidobacteria subgroup.

that taken from the Yarqon streambed (supporting information Text S2 and Figures 4a and 4b). The dominant bacterial phylum that constituted the biofilms was Proteobacteria, accounting for more than 48% of the total operational taxonomic units (OTUs). Within that phylum, α, β, and γ Proteobacteria classes accounted for 11% ± 1, 22% ± 3, and 10% ± 2, respectively. In these biofilms, the Planctomycetia, Anaerolineae, and Saprospirae classes were also found to be highly abundant, ranging from 5% to 8% of the total OTUs. In contrast, in the stationary bed forms, in which the sediment was undisturbed for about 2 months, the biofilm community structure was found to differ between the stoss and lee sides (Figures 4c and 4d). Regardless of these conditions, and similar to the disturbed bed forms, α and β Proteobacteria were still the dominant classes and accounted for 13% ± 1 and 27% ± 2 of the total OTUs, respectively. However, in the downstream location, we found that the biofilms comprised a highly diverse community structure with additional classes including Cytophagia, Saprospirae, Sphingobacteriia, and Acidobacteria (Figure 4d).

By incorporating all the information from the results, it was evident that various factors may affect oxygen consumption. Distinct patterns include the observations that the values of both the bacterial production

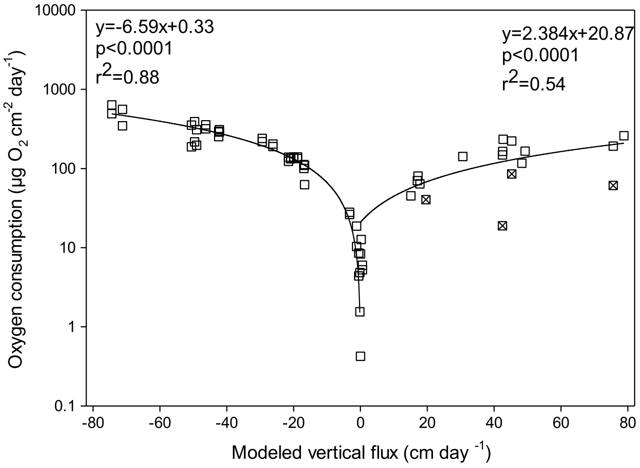

Figure 5. The relationship between the vertical water fluxes and oxygen consumption rates. Vertical fluxes represent the net upwelling or downwelling fluxes that resulted from the combination of hyporheic flow and losing or gaining flow conditions. Consumption rates with a fit that yielded an r^2 of less than 0.5 are marked with an x.

rates and the cell-specific activity spanned over 1 order of magnitude (Figure 3), while the oxygen consumption rates spanned over 4 orders of magnitude (Table 1). To further explore these relationships, we conducted a multiple regression analysis between the oxygen consumption rates, the hydrological factors, and the microbial parameters. It was found that the modeled vertical fluxes have a much stronger explanatory power on the oxygen consumption rates (AIC score of 472.5) than the predictive power of the model that includes all the hydrological and the microbial parameters together (AIC score of 479.3). This is also shown in Figure 5 and supporting information Text S3.

4. Discussion

4.1. Linking Microbial and Hydrological Processes

The results of this study indicate that there is not always a direct link between bacterial abundance and activity (Figure 3). This phenomenon was also observed in other studies (e.g., Yanuka-Golub et al., 2014) and can be explained by the physiological status of the microorganisms. Under stress, for example, under toxic conditions or chemical gradients (e.g., Stewart & Franklin, 2008) or under successional stage (e.g., Sekar et al., 2002), bacteria may reallocate metabolic resources from growth to the production of protective molecules. Such a change will directly affect reaction rates and may ultimately translate into a shift in the community structure (DeAngelis et al., 2010; Schimel et al., 2007). Our results indicate that the biofilm community structure in the Yarqon streambed and in our experimental flume was dominated by α and β Proteobacteria, as well as γ and δ Proteobacteria, regardless of the flow and sedimentary conditions as opposed to the hypothesis (Figure 4). These bacterial classes, which were found to be highly common in various stream sediments (e.g., Battin et al., 2016), are mostly facultative or obligatory anaerobes that are highly adaptable to a broad range of metabolic strategies. However, as the sediment became stationary, additional classes were found to constitute the biofilm at the lee side of the bed form (Figure 4d). It is likely that various microenvironments were formed under these steady conditions, enabling specific bacterial classes to colonize them and form biofilms. We suggest that photosynthetic classes such as Acidobacteria (represented in the study by the Chloracidobacteria subgroup) would be found in the top sediment layers (Bína et al., 2016; Teramura et al., 2018), whereas Anaerolineae would form biofilms in deeper layers where anaerobic conditions prevail (Abed et al., 2014). In addition, we postulate that other classes such as Sphingobacteriia would become dominant over time if conditions remain stable, as was previously found in other ecosystems (da Costa et al., 2018; Siles & Margesin, 2018). Nevertheless, it is likely that even after such a community shift and adjustments to new environmental conditions, the overall oxygen consumption would not be drastically modified. Similar to other studies, we surmise that regardless of the changes in the microbial community, the utilization of nutrients would be relatively constant across seasons and the spatial location within the stream network, following the River Continuum Concept (Battin et al., 2008; Vannote et al., 1980).

Quantifying the links between flow dynamics, bacterial community, and oxygen consumption is partially limited by the inability to measure the dynamic nature of microbial abundance and community structure (mostly requiring disruptive sampling). Special efforts were also made here to collect information on bacterial abundance; however, the multiple regression analysis did not reveal any significant trend-linking oxygen consumption and bacterial parameters such as abundance or bacterial production. These results are similar to the findings of Higashino (2013), and thus, we suggest that there was no link between oxygen consumption and bacterial abundance and that the supply of oxygen from the exchange flow determined the oxygen consumption rates.

The results of this study indicate that hydrological processes can provide descriptive information supporting the modeling of oxygen dynamics in eutrophic-sandy streambeds, which was mimicked in our experiments by supplying nutrients above limiting levels, as are often found in agriculture- and urban-impacted streams. We also show that increasing the overlying velocity positively affected the consumption rates, but most of the changes were bound to the same order of magnitude (Table 1). This is important because it shows that the exchange flux, which determines oxygen consumption, was dominated by losing and gaining fluxes and not by the overlying water velocity despite the fact that the hyporheic exchange flux scales with the square of the stream water velocity (Arnon et al., 2013; Packman & Brooks, 2001).

Reeder et al. (2018) demonstrated recently that oxygen consumption rates can be quantified as a function of the oxygen downwelling flux. While the aforementioned study was conducted under neutral conditions, our results suggest that additional information can be obtained by the ability to evaluate the net vertical exchange flux between the water and the sediment also when losing or gaining fluxes are involved (Table 1). The strong influence of losing and gaining fluxes on hyporheic exchange implies that the magnitude of these fluxes is very important. The range of fluxes that we used in our study represents high flux levels (e.g., 50 cm/day) and the fluxes of 20 cm/day that are well within the commonly reported levels (e.g., Hünken & Mutz, 2007; Mutz & Rohde, 2003; Stofleth et al., 2007; Strommer & Smock, 1989).

To further illustrate the dependence of oxygen consumption rates on the vertical flux, we changed the vertical flux that was used for calculating the data for Figure 5 by ±30% and recalculated the oxygen consumption rates. This was done to reflect potential error in the modeled vertical flux and its effect on oxygen consumption. We found that in all cases with a strong upwelling/downwelling flux, a ±30% error in the flux resulted in approximately ±30% variations in the oxygen consumption rates (supporting information Text S4). These results indicate that oxygen consumption is directly proportional to the upwelling/downwelling flux. Under neutral conditions, oxygen supply to the streambed was less influenced by the change in the flux, and the change in the oxygen consumption rate was, in general, smaller than 30%. These results indicate that the system was mostly transport limited, and as such, we expect the results to follow the trends described in Figure 5. Our estimation of fluxes along the bed forms is consistent with the majority of previous studies (assuming that flux varies because of hydraulic head variations) and captures most of the spatial variability along these bed forms (Boano et al., 2008; Cardenas & Wilson, 2007; Elliott & Brooks, 1997). Even though some residual bias may still be present, the range of the calculated vertical flux is expected to be correct. We deduce that even a small relative error, which may lead to under/overestimation of oxygen consumption rates, is negligible compared to the change that was observed in the oxygen consumption rates (Figure 5). Although hyporheic exchange was not measured directly in these experiments, our previous study suggests that the imposed fluxes used here suppressed the hyporheic exchange to a level that makes its impact negligible as compared to the imposed fluxes (Fox et al., 2014).

It is important to note that using a 1-D model simplifies the real flow patterns, which are 2-D in nature for the case presented here and 3-D for most field cases. Nevertheless, a modeling study by Boano et al. (2018) used several oxygen profiles that were collected within the same sediments to show that the differences between the oxygen consumption rates that were calculated by the GRADIENT model and those calculated by a 2-D model were relatively small. It was found that the results by GRADIENT were, on average, 8% lower (and ranged between +5% and −25% depending on the magnitude of the horizontal flux). The fact that oxygen consumption rates in our study spanned over 4 orders of magnitude implies that the simplification of using a 1-D model did not bias the patterns shown in Figure 5. The results suggest that hydrological conditions can explain and can be used for predicting oxygen consumption rates without explicitly considering the bacterial community structure in sandy streambeds under nutrient-rich conditions. This is especially relevant in situations such as that portrayed here when the system is transport limited.

4.2. Implications for Biogeochemical Processes in Streams

Transferring these findings from experimental and modeling efforts to actual field conditions constitutes the next natural step. Combining controlled laboratory experiments and numerical modeling enabled us to show that under nutrient-rich conditions, oxygen consumption rates depend primarily on the net vertical exchange flux between the water and the streambed. Concomitant with the above, the distribution of bacterial biomass was shown to have a secondary influence. We suggest that the focus on fluxes rather than on biomass could be valid when bacterial abundance varies within 1 order of magnitude between habitats, which is common in many streams (Cardinale et al., 2002; Fischer et al., 2002, 2003). While other studies noticed a positive effect of water fluxes on stream metabolism (González-Pinzón et al., 2014; Vieweg et al., 2016), they mostly focused on the effect of overlying water velocity and only rarely looked at the interaction with the groundwater (e.g., Argerich et al., 2011). However, no significant efforts were made to evaluate the local downwelling/upwelling flux-consumption relationship and how this may affect the overall metabolism. Instead, efforts were made to find the link between residence time distributions and oxygen consumption rates. Residence times may be important in cases in which incomplete consumption of oxygen occurs and the extent of the oxic zone and oxic-anoxic zonation is significant (Zarnetske et al., 2011). Such information may be less important for aerobic metabolism but very important for anaerobic processes, such as denitrification.

The relationship between oxygen consumption and vertical flux that was found here indicates that even under gaining conditions, there may be an increase in the oxygen consumption rate although the general notion is that groundwater is depleted in oxygen. However, the oxygen concentration in upwelling groundwater spans over a wide range of concentrations as reviewed by Malard and Hervant (1999) and recently reported in studies on the hyporheic zone (e.g., Krause et al., 2013). We surmise that the variability of the data and the lower goodness of fit under gaining conditions, compared to under losing conditions, occurred due to the fact that the amount of oxygen that reached the upper section of the bed was hard to control under these conditions (Table 1). It is reasonable to assume that for various field cases, the effect of upwelling fluxes on oxygen consumption should be less pronounced than what was shown here in cases of low oxygen concentrations in the upwelling groundwater. Regardless of the oxygen flux from the upwelling water, gaining conditions reduced the size of the active hyporheic zone as is nicely shown in Figure 2, as well as in other studies (Fox et al., 2016; Trauth et al., 2013). These findings suggest that it is important to specifically measure the oxygen concentrations in the aquifer in the case of gaining conditions because they may strongly affect the estimation of respiration in the hyporheic zone.

Various studies suggest that the estimation of residence time distribution in the hyporheic zone can be used to quantify biogeochemical processes (e.g., Gomez et al., 2012; Reeder et al., 2018; Zarnetske et al., 2011). However, estimation of residence time distribution requires extensive modeling efforts, especially when a 3-D flow configuration is considered. This requirement may limit the ability to perform the evaluation at the field scale due to the efforts and skills needed to achieve a comprehensive model, even at the local scale. However, measuring the local vertical flux at specific locations in the streambed is now possible with emerging new technologies, such as heat pulse sensors (Angermann et al., 2012), seepage meters (Solder et al., 2015), and the more traditional methods of hydraulic head measurements in standpipes (e.g., Chen et al., 2009). Extending the local measurements to a larger scale is possible by applying the spatial information from the patch scale to the reach scale as was recently discussed in several publications (e.g., Krause et al., 2013; McClain et al., 2003; Peipoch et al., 2016; Pinay et al., 2015). Similar works that combine vertical fluxes with information on biomass and biogeochemical reaction rates are difficult to execute and therefore not common (De Falco et al., 2016; Li et al., 2017; Mendoza-Lera & Datry, 2017; Mendoza-Lera & Mutz, 2013; Reeder et al., 2018), thus hindering the extension of our findings to the reach scales and beyond. More data on the spatial distribution of biomass, vertical fluxes, and local biogeochemical reaction rates are needed for a more conclusive recommendation on model parametrization and for developing methods to extend the small-scale distributions (and hot spots) to the reach and network scales of various stream types.

Acknowledgments
This research was supported by the Israel Science Foundation (grant 682/17) and by a grant (Israel-Italy Joint Innovation Program for Scientific and Technological Cooperation in R&D) from the Israeli Ministry of Science, Technology and Space and the Italian Ministry of Foreign Affairs, Directorate General for Political and Security Affairs. We thank Hila Frank and Chen Hargil for laboratory assistance and Samara Bel for editorial assistance. The data of the experiments are provided in the table within the text and in the supporting information.

References

Abed, R. M. M., Al-Kindi, S., & Al-Kharusi, S. (2014). Diversity of bacterial communities along a petroleum contamination gradient in desert soils. *Microbial Ecology*, *69*(1), 95–105. https://doi.org/10.1007/s00248-014-0475-5

Akaike, H. (1973). Maximum likelihood identification of Gaussian autoregressive moving average models. *Biometrika*, *60*(2), 255–265. https://doi.org/10.1093/biomet/60.2.255

Angermann, L., Lewandowski, J., Fleckenstein, J. H., & Nützmann, G. (2012). A 3D analysis algorithm to improve interpretation of heat pulse sensor results for the determination of small-scale flow directions and velocities in the hyporheic zone. *Journal of Hydrology*, *475*, 1–11. https://doi.org/10.1016/j.jhydrol. 2012.06.050

Argerich, A., Martí, E., Sabater, F., & Ribot, M. (2011). Temporal variation of hydrological exchange and hyporheic biogeochemistry in a headwater stream during autumn. *Journal of the North American Benthological Society*, *30*(3), 635–652. https://doi.org/10.1899/10-078.1

Arnon, S., Avni, N., & Gafny, S. (2015). Nutrient uptake and macroinvertebrate community structure in a highly regulated Mediterranean stream receiving treated wastewater. *Aquatic Sciences*, *77*(4), 623–637. https://doi.org/10.1007/s00027-015-0407-6

Arnon, S., Gray, K. A., & Packman, A. I. (2007). Biophysicochemical process coupling controls nitrogen use by benthic biofilms. *Limnology and Oceanography*, *52*(4), 1665–1671. https://doi.org/10.4319/lo. 2007.52.4.1665

Arnon, S., Yanuka, K., & Nejidat, A. (2013). Impact of overlying water velocity on ammonium uptake by benthic biofilms. *Hydrological Processes*, *27*(4), 570–578. https://doi.org/10.1002/hyp.9239

Aubeneau, A. F., Hanrahan, B., Bolster, D., & Tank, J. (2016). Biofilm growth in gravel bed streams controls solute residence time distributions. *Journal of Geophysical Research: Biogeosciences*, *121*, 1840–1850. https://doi.org/10.1002/2016JG003333

Bardini, L., Boano, F., Cardenas, M. B., Revelli, R., & Ridolfi, L. (2012). Nutrient cycling in bedform induced hyporheic zones. *Geochimica et Cosmochimica Acta*, *84*, 47–61. https://doi.org/10.1016/j.gca. 2012.01.025

Battin, T. J., Besemer, K., Bengtsson, M. M., Romani, A. M., Packmann, A. I., Packman, A. I., & Packmann, A. I. (2016). The ecology and biogeochemistry of stream biofilms. *Nature Reviews Microbiology*, *14*(4), 251–263. https://doi.org/10.1038/nrmicro.2016.15

Battin, T. J., Kaplan, L. A., Findlay, S., Hopkinson, C. S., Marti, E., Packman, A. I., et al. (2008). Biophysical controls on organic carbon fluxes in fluvial networks. *Nature Geoscience*, *2*(8), 595–100. https://doi.org/10.1038/ngeo602

Baveye, P., Vandevivere, P., Hoyle, B. L., DeLeo, P. C., & Sanchez De Lozada, D. (1998). Environmental impact and mechanisms of the biological clogging of saturated soils and aquifer materials. *Critical Reviews in Environmental Science and Technology*, *28*(2), 123–191. https://doi.org/10.1080/10643389891254197

Bencala, K. E., & Walters, R. A. (1983). Simulation of solute transport in a mountain pool-and-riffle stream: A transient storage model. *Water Resources Research*, *19*(3), 718–724. https://doi.org/10.1029/WR019i003p00718

Berg, P., Risgaard-Petersen, N., & Rysgaard, S. S. (1998). Interpretation of measured concentration profiles in sediment pore water. *Limnology and Oceanography*, *43*(7), 1500–1510. https://doi.org/10.4319/lo. 1998.43.7.1500

Besemer, K., Peter, H., Logue, J. B., Langenheder, S., Lindström, E. S., Tranvik, L. J., & Battin, T. J. (2012). Unraveling assembly of stream biofilm communities. *ISME Journal*, *6*(8), 1459–1468. https://doi.org/10.1038/ismej. 2011.205

Besemer, K., Singer, G., Limberger, R., Chlup, A.-K. K., Hochedlinger, G., Hodl, I., et al. (2007). Biophysical controls on community succession in stream biofilms. *Applied and Environmental Microbiology*, *73*(15), 4966–4974. https://doi.org/10.1128/AEM.00588-07

Bína, D., Gardian, Z., Vácha, F., & Litvín, R. (2016). Native FMO-reaction center supercomplex in green sulfur bacteria: An electron microscopy study. *Photosynthesis Research*, *128*(1), 93–102. https://doi.org/10.1007/s11120-015-0205-y

Boano, F., De Falco, N., & Arnon, S. (2018). Modeling chemical gradients in sediments under losing and gaining flow conditions: The GRADIENT code. *Advances in Water Resources*, *112*, 72–82. https://doi.org/10.1016/j.advwatres. 2017.12.002

Boano, F., Harvey, J. W., Marion, A., Packman, A. I., Revelli, R., Ridolfi, L., & Wörman, A. (2014). Hyporheic flow and transport processes: Mechanisms, models, and biogeochemical implications. *Reviews of Geophysics*, *52*, 603–679. https://doi.org/10.1002/2012RG000417

Boano, F., Revelli, R., & Ridolfi, L. (2008). Reduction of the hyporheic zone volume due to the stream-aquifer interaction. *Geophysical Research Letters*, *35*, L09401. https://doi.org/10.1029/2008GL033554

Boulton, A. J., Datry, T., Kasahara, T., Mutz, M., & Stanford, J. A. (2010). Ecology and management of the hyporheic zone: Stream–groundwater interactions of running waters and their floodplains. *Journal of North American Benthological Society*, *29*(1), 26–40. https://doi.org/10.1899/08-017.1

Boulton, A. J., Findlay, S., Marmonier, P., Stanley, E. H., & Valett, H. M. (1998). The functional significance of the hyporheic zone in streams and rivers. *Annual Review of Ecology and Systematics*, *29*(1), 59–81. https://doi.org/10.1146/annurev.ecolsys.29.1.59

Cardenas, M. B. (2009). Stream-aquifer interactions and hyporheic exchange in gaining and losing sinuous streams. *Water Resources Research*, *45*, W06429. https://doi.org/10.1029/2008wr007651

Cardenas, M. B. (2015). Hyporheic zone hydrologic science: A historical account of its emergence and a prospectus. *Water Resources Research*, *51*, 3601–3616. https://doi.org/10.1002/2015WR017028

Cardenas, M. B., & Wilson, J. L. (2007). Exchange across a sediment–water interface with ambient groundwater discharge. *Journal of Hydrology*, *346*(3–4), 69–80. https://doi.org/10.1016/j.jhydrol.2007.08.019

Cardinale, B. J., Palmer, M. A., Swan, C. M., Brooks, S., Poff, N. L., & Feb, N. (2002). The influence of substrate heterogeneity on biofilm metabolism in a stream ecosystem. *Ecology*, *83*(2), 412–422. https://doi.org/10.1890/0012-9658(2002)083[0412:TIOSHO]2.0.CO;2

Caruso, A., Boano, F., Ridolfi, L., Chopp, D. L., & Packman, A. (2017). Biofilm-induced bioclogging produces sharp interfaces in hyporheic flow, redox conditions, and microbial community structure. *Geophysical Research Letters*, *44*, 4917–4925. https://doi.org/10.1002/2017GL073651

Chen, X., Song, J., Cheng, C., Wang, D., & Lackey, S. O. (2009). A new method for mapping variability in vertical seepage flux in streambeds. *Hydrogeology Journal*, *17*(3), 519–525. https://doi.org/10.1007/s10040-008-0384-0

da Costa, D. P., Dias, A. C. F., Cotta, S. R., Vilela, D., de Andrade, P. A. M., Pellizari, V. H., & Andreote, F. D. (2018). Changes of bacterial communities in the rhizosphere of sugarcane under elevated concentration of atmospheric CO2. *Global Change Biology Bioenergy*, *10*(2), 137–145. https://doi.org/10.1111/gcbb. 12476

De Falco, N., Boano, F., & Arnon, S. (2016). Biodegradation of labile dissolved organic carbon under losing and gaining streamflow conditions simulated in a laboratory flume. *Limnology and Oceanography*, *61*(5), 1839–1852. https://doi.org/10.1002/lno.10344

DeAngelis, K. M., Silver, W. L., Thompson, A. W., & Firestone, M. K. (2010). Microbial communities acclimate to recurring changes in soil redox potential status. *Environmental Microbiology*, *12*(12), 3137–3149. https://doi.org/10.1111/j.1462-2920.2010.02286.x

Elliott, H., & Brooks, N. H. (1997). Transfer of nonsorbing solutes to a streambed with bed forms: Laboratory experiments. *Water Resources Research*, *33*(1), 137–151. https://doi.org/10.1029/96WR02783

Fischer, H., Sachse, A., Steinberg, C. E. W., & Pusch, M. (2002). Differential retention and utilization of dissolved organic carbon by bacteria in river sediments. *Limnology and Oceanography*, *47*(6), 1702–1711. https://doi.org/10.4319/lo.2002.47.6.1702

Fischer, H., Sukhodolov, A., Wilczek, S., & Engelhardt, C. (2003). Effects of flow dynamics and sediment movement on microbial activity in a lowland River. *River Research and Applications*, *19*(5–6), 473–482. https://doi.org/10.1002/rra.731

Flury, S., Glud, R. N., Premke, K., & McGinnis, D. F. (2015). Effect of sediment gas voids and ebullition on benthic solute exchange. *Environmental Science and Technology*, *49*(17), 10413–10420. https://doi.org/10.1021/acs.est.5b01967

Fox, A., Boano, F., & Arnon, S. (2014). Impact of losing and gaining streamflow conditions on hyporheic exchange fluxes induced by dune-shaped bed forms. *Water Resources Research*, *50*, 1895–1907. https://doi.org/10.1002/2013WR014668

Fox, A., Laube, G., Schmidt, C., Fleckenstein, J. H., & Arnon, S. (2016). The effect of losing and gaining flow conditions on hyporheic exchange in heterogeneous streambeds. *Water Resources Research*, *51*, 1333–1352. https://doi.org/10.1002/2014WR015716

Fox, A., Packman, A. I., Boano, F., Colin, B. P., & Arnon, S. (2018). Interactions between suspended kaolinite deposition and hyporheic exchange flux under losing and gaining flow conditions. *Geophysical Research Letters*, *45*, 4077–4085. https://doi.org/10.1029/2018GL077951

Frank, H., Rahav, E., & Bar-Zeev, E. (2017). Short-term effects of SWRO desalination brine on benthic heterotrophic microbial communities. *Desalination*, *417*, 52–59. https://doi.org/10.1016/j.desal.2017.04.031

Gerull, L., Frossard, A., Gessner, M. O., & Mutz, M. (2012). Effects of shallow and deep sediment disturbance on whole-stream metabolism in experimental sand-bed flumes. *Hydrobiologia*, *683*(1), 297–310. https://doi.org/10.1007/s10750-011-0968-x

Gomez, J. D., Wilson, J. L., & Cardenas, M. B. (2012). Residence time distributions in sinuosity-driven hyporheic zones and their biogeochemical effects. *Water Resources Research*, *48*, W09533. https://doi.org/10.1029/2012WR012180

Gomez-velez, J. D., & Harvey, J. W. (2014). A hydrogeomorphic river network model predicts where and why hyporheic exchange is important in large basins. *Geophysical Research Letters*, *41*, 6403–6412. https://doi.org/10.1002/2014GL061099

Gomez-Velez, J. D., Harvey, J. W., Cardenas, M. B., & Kiel, B. (2015). Denitrification in the Mississippi River network controlled by flow through river bedforms. *Nature Geoscience*, *8*(12), 941–945. https://doi.org/10.1038/ngeo2567

González-Pinzón, R., Haggerty, R., & Argerich, A. (2014). Quantifying spatial differences in metabolism in headwater streams. *Freshwater Science*, *33*(3), 798–811. https://doi.org/10.1086/677555

Higashino, M. (2013). Quantifying a significance of sediment particle size to hyporheic sedimentary oxygen demand with a permeable stream bed. *Environmental Fluid Mechanics*, *13*(3), 227–241. https://doi.org/10.1007/s10652-012-9262-3

Hödl, I., Mari, L., Bertuzzo, E., Suweis, S., Besemer, K., Rinaldo, A., & Battin, T. J. (2013). Biophysical controls on cluster dynamics and architectural differentiation of microbial biofilms in contrasting flow environments. *Environmental Microbiology*, *16*(3), 802–812. https://doi.org/10.1111/1462-2920.12205

Hünken, A., & Mutz, M. (2007). Field studies on factors affecting very fine and ultra fine particulate organic matter deposition in low-gradient sand-bed streams. *Hydrological Processes*, *21*(4), 525–533. https://doi.org/10.1002/hyp.6263

Klute, A., & Dirksen, C. (1986). Hydraulic conductivity and diffusivity: Laboratory methods. In A. Klute (Ed.), *Methods of Soil Analysis. Part 1. Physical and Mineralogical Methods* (2nd ed., pp. 687–734). Madison, WI: Agron. Monogr. 9. ASA. https://doi.org/10.2136/sssabookser5.1.2ed.c30

Krause, S., Tecklenburg, C., Munz, M., & Naden, E. (2013). Streambed nitrogen cycling beyond the hyporheic zone: Flow controls on horizontal patterns and depth distribution of nitrate and dissolved oxygen in the upwelling groundwater of a lowland river. *Journal of Geophysical Research: Biogeosciences*, *118*, 54–67. https://doi.org/10.1029/2012JG002122

Li, A., Aubeneau, A. F., Bolster, D., Tank, J. L., & Packman, A. I. (2017). Covariation in patterns of turbulence-driven hyporheic flow and denitrification enhances reach-scale nitrogen removal. *Water Resources Research*, *53*, 6927–6944. https://doi.org/10.1002/2016WR019949

Malard, F., & Hervant, F. (1999). Oxygen supply and adaptation of animals in groundwater. *Freshwater Biology*, *41*(1), 1–30. https://doi.org/10.1046/j.1365-2427.1999.00379.x

Marx, A., Dusek, J., Jankovec, J., Hartmann, J., & Barth, J. A. C. (2017). A review of CO_2 and associated carbon dynamics in headwater streams: A global perspective. *Reviews of Geophysics*, *55*, 560–585. https://doi.org/10.1002/2016RG000547

Mathers, K. L., Millett, J., Robertson, A. L., Stubbington, R., & Wood, P. J. (2014). Faunal response to benthic and hyporheic sedimentation varies with direction of vertical hydrological exchange. *Freshwater Biology*, *59*(11), 2278–2289. https://doi.org/10.1111/fwb. 12430

McClain, M. E., Boyer, E. W., Dent, C. L., Gergel, S. E., Grimm, N. B., Groffman, P. M., et al. (2003). Biogeochemical hot spots and hot moments at the interface of terrestrial and aquatic ecosystems. *Ecosystems*, *6*(4), 301–312. https://doi.org/10.1007/s10021-003-0161-9

Mendoza-lera, C., & Datry, T. (2017). Relating hydraulic conductivity and hyporheic zone biogeochemical processing to conserve and restore river ecosystem services. *Science of the Total Environment*, *579*, 1815–1821. https://doi.org/10.1016/j.scitotenv.2016.11.166

Mendoza-Lera, C., Frossard, A., Knie, M., Federlein, L. L., Gessner, M. O., & Mutz, M. (2017). Importance of advective mass transfer and sediment surface area for streambed microbial communities. *Freshwater Biology*, *62*(1), 133–145. https://doi.org/10.1111/fwb.12856

Mendoza-Lera, C., & Mutz, M. (2013). Microbial activity and sediment disturbance modulate the vertical water flux in sandy sediments. *Freshwater Science*, *32*(1), 26–38. https://doi.org/10.1899/11-165.1

Mutz, M., & Rohde, A. (2003). Processes of surface-subsurface water exchange in a low energy sand-bed stream. *International Review of Hydrobiology*, *88*(34), 290–303. https://doi.org/10.1002/iroh.200390026

Newcomer, M. E., Hubbard, S. S., Fleckenstein, J. H., Maier, U., Schmidt, C., Thullner, M., et al. (2018). Influence of hydrological perturbations and riverbed sediment characteristics on hyporheic zone respiration of CO_2 and N_2. *Journal of Geophysical Research: Biogeosciences*, *123*, 902–922. https://doi.org/10.1002/2017JG004090

Nogaro, G., Mermillod-Blondin, F., François-Carcaillet, F., Gaudet, J. P., Lafont, M., & Gibert, J. (2006). Invertebrate bioturbation can reduce the clogging of sediment: An experimental study using infiltration sediment columns. *Freshwater Biology*, *51*(8), 1458–1473. https://doi.org/10.1111/j.1365-2427.2006.01577.x

Packman, A., Salehin, M., & Zaramella, M. (2004). Hyporheic exchange with gravel beds: Basic hydrodynamic interactions and bedform-induced advective flows. *Journal of Hydraulic Engineering*, *130*(7), 647–656. https://doi.org/10.1061/(ASCE)0733-9429(2004)130:7(647)

Packman, A. I., & Brooks, N. H. (2001). Hyporheic exchange of solutes and colloids with moving bed forms. *Water Resources Research*, *37*(10), 2591–2605. https://doi.org/10.1029/2001WR000477

Partington, D., Therrien, R., Simmons, C. T., & Brunner, P. (2017). Blueprint for a coupled model of sedimentology, hydrology, and hydrogeology in streambeds. *Reviews of Geophysics*, *55*, 287–309. https://doi.org/10.1002/2016RG000530

Peipoch, M., Gacia, E., Bastias, E., Serra, A., Proia, L., Ribot, M., et al. (2016). Small-scale heterogeneity of microbial N uptake in streams and its implications at the ecosystem level. *Ecology*, *97*(5), 1329–1344. https://doi.org/10.1890/15-1210.1

Pinay, G., Peiffer, S., De Dreuzy, J. R., Krause, S., Hannah, D. M., Fleckenstein, J. H., et al. (2015). Upscaling nitrogen removal capacity from local hotspots to low stream orders' drainage basins. *Ecosystems*, *18*(6), 1101–1120. https://doi.org/10.1007/s10021-015-9878-5

Raymond, P. A., Hartmann, J., Lauerwald, R., Sobek, S., McDonald, C., Hoover, M., et al. (2013). Global carbon dioxide emissions from inland waters. *Nature*, *503*(7476), 355–359. https://doi.org/10.1038/nature12760

Reeder, W. J., Quick, A. M., Farrell, T. B., Benner, S. G., Feris, K. P., & Tonina, D. (2018). Spatial and temporal dynamics of dissolved oxygen concentrations and bioactivity in the hyporheic zone. *Water Resources Research*, *54*, 2112–2128. https://doi.org/10.1002/2017WR021388

Risse-Buhl, U., Anlanger, C., Kalla, K., Neu, T. R., Noss, C., Lorke, A., & Weitere, M. (2017). The role of hydrodynamics in shaping the composition and architecture of epilithic biofilms in fluvial ecosystems. *Water Research*, *127*, 211–222. https://doi.org/10.1016/j.watres. 2017.09.054

Samsó, R., García, J., Molle, P., & Forquet, N. (2016). Modelling bioclogging in variably saturated porous media and the interactions between surface/subsurface flows: Application to constructed wetlands. *Journal of Environmental Management*, *165*, 271–279. https://doi.org/10.1016/j.jenvman.2015.09.045

Schimel, J., Balser, T. C., & Wallenstein, M. (2007). Microbial stress-response physiology and its implications for ecosystem function. *Ecology*, *88*(6), 1386–1394. https://doi.org/10.1890/06-0219

Sekar, R., Nair, K. V. K., Rao, V. N. R., & Venugopalan, V. P. (2002). Nutrient dynamics and successional changes in a lentic freshwater biofilm. *Freshwater Biology*, *47*(10), 1893–1907. https://doi.org/10.1046/j.1365-2427.2002.00936.x

Siles, J. A., & Margesin, R. (2018). Insights into microbial communities mediating the bioremediation of hydrocarbon-contaminated soil from an Alpine former military site. *Applied Microbiology and Biotechnology*, *102*(10), 4409–4421. https://doi.org/10.1007/s00253-018-8932-6

Simon, M., & Azam, F. (1989). Protein content and protein synthesis rates of planktonic marine bacteria. *Marine Ecology Progress Series*, *51*, 201–213. https://doi.org/10.3354/meps051201

Smith, D. C., & Azam, F. (1992). A simple, economical method for measuring bacterial protein synthesis rates in seawater using 3H-leucine. *Marine Microbial Food Webs*, *6*(2), 107–114.

Solder, J. E., Gilmore, T. E., Genereux, D. P., & Solomon, D. K. (2015). A tube seepage meter for in situ measurement of seepage rate and groundwater sampling. *Groundwater*, *54*(4), 588–595. https://doi.org/10.1111/gwat.12388

Stewart, P. S., & Franklin, M. J. (2008). Physiological heterogeneity in biofilms. *Nature Reviews Microbiology*, *6*(3), 199–210. https://doi.org/10.1038/nrmicro1838

Stofleth, J. M., Douglas Shields, F., & Fox, G. A. (2007). Hyporheic and total transient storage in small, sand-bed streams. *Hydrological Processes*, *22*(12), 1885–1894. https://doi.org/10.1002/hyp.6773

Strommer, J., & Smock, L. A. (1989). Vertical distribution and abundance of invertebrates within the sandy substrate of a low-gradient headwater stream. *Freshwater Biology*, *22*(2), 263–274. https://doi.org/10.1111/j.1365-2427.1989.tb01099.x

Teramura, M., Harada, J., & Tamiaki, H. (2018). In vitro enzymatic assays of photosynthetic bacterial 3-vinyl hydratases for bacteriochlorophyll biosyntheses. *Photosynthesis Research*, *135*(1–3), 319–328. https://doi.org/10.1007/s11120-017-0415-6

Trauth, N., Schmidt, C., Maier, U., Vieweg, M., & Fleckenstein, J. H. (2013). Coupled 3D stream flow and hyporheic flow model under varying stream and ambient groundwater flow conditions in a pool-riffle system. *Water Resources Research*, *49*, 5834–5850. https://doi.org/10.1002/wrcr.20442

Vannote, R. L., Minshall, G. W., Cummins, K. W., Sedell, J. R., & Cushing, C. E. (1980). The river continuum concept. *Canadian Journal of Fisheries and Aquatic Sciences*, *37*(1), 130–137. https://doi.org/10.1139/f80-017

Vieweg, M., Kurz, M. J., Trauth, N., Fleckenstein, J. H., Musolff, A., & Schmidt, C. (2016). Estimating time-variable aerobic respiration in the streambed by combining electrical conductivity and dissolved oxygen time series. *Journal of Geophysical Research: Biogeosciences*, *121*, 2199–2215. https://doi.org/10.1002/2016JG003345

Yanuka-Golub, K., Arnon, S., & Nejidat, A. (2014). Impact of streambed morphology on the abundance and activity of ammonia-oxidizing bacteria. *FEMS Microbiology Ecology*, *90*(1), 175–183. https://doi.org/10.1111/1574-6941.12385

Zarnetske, J. P., Haggerty, R., Wondzell, S. M., & Baker, M. a. (2011). Dynamics of nitrate production and removal as a function of residence time in the hyporheic zone. *Journal of Geophysical Research*, *116*, G01025. https://doi.org/10.1029/2010JG001356

Zscheischler, J., Mahecha, M. D., Avitabile, V., Calle, L., & Carvalhais, N. (2017). Reviews and syntheses: An empirical spatiotemporal description of the global surface-atmosphere carbon fluxes: Opportunities and data limitations. *Biogeosciences*, *14*(15), 3685–3703. https://doi.org/10.5194/bg-14-3685-2017